

## Integration of observations for detection of aircraft icing conditions during AIRS2: Comparisons of microphysical parameters

I. Gultepe<sup>1,2</sup>, G. A. Isaac<sup>2</sup>, P. Minnis<sup>3</sup>, J. K. Ayers<sup>4</sup>

<sup>2</sup>Cloud Physics and Severe Weather Research Division  
Environment Canada, Toronto, Ontario M3H 5T4

<sup>3</sup>MS 420, NASA Langley Research Center  
Hampton, VA 23681-0001

<sup>4</sup>Analytical Services and Materials, Inc.  
One Enterprise Parkway, Hampton, VA 23666

### 1. INTRODUCTION

Mixed phase clouds contain both liquid and ice particles at various scales along which the liquid fraction is highly variable and depends on physical, dynamical, and nucleation processes. Because of the smaller saturation vapor pressure over ice crystals compared to liquid droplets, ice crystals glaciate clouds in short time periods at the expense of droplets. In numerical models, droplet number concentration ( $N_d$ ) is usually assumed to be constant sometimes resulting in a large uncertainty in mixed phase cloud representation (Gultepe and Isaac, 2004). For this reason, icing processes should be better understood. The Alliance Icing Research Study (AIRS1, Isaac et al., 2001) that took place over southern Ontario and Quebec during the winter of 1999-2000 was a major icing research program. The AIRS2 field program, which followed AIRS1 and AIRS1.5, was designed to study large-scale icing environment characteristics and develop airport warning systems for icing and hazardous winter conditions (Isaac et al., 2005a). Analyses of satellite imager data, especially from the Geostationary Operational Environmental Satellites (GOES) have the potential for timely large-scale characterization of icing conditions in many instances (e.g., Minnis et al., 2004), but further examination and refinement of the satellite

analyses are needed to improve the reliability of satellite algorithms. By combining satellite and aircraft measurements, it should be possible to enhance our understanding of the icing environment. Thus, GOES data were analyzed throughout AIRS2, which was conducted from 2 November 2003 through 27 February 2004 in the same location as AIRS1.

In this work, microphysical parameters obtained using aircraft observations are compared with satellite-based retrievals along the flight tracks and in a fixed area (e.g. Mirabel) over 1257 km<sup>2</sup>, representing 20-km radius. A total of 22 flights were used in the analysis. Then, these comparisons are discussed to emphasize the importance of integrated observations (Gultepe et al., 2004).

### 2. OBSERVATIONS AND MODEL DATA

Observations at the surface were collected at the Mirabel test-bed site, which included various conventional, optical, and remote sensing instruments. Other measurements were made using aircraft and satellite observations. When clouds with liquid were expected, a flight was executed over the test site. Otherwise, in-situ data were collected in the vicinity of the project area where liquid clouds were found.

#### 2.1 In-situ Observations

In-situ observations were collected with instruments mounted on the National Research Council (NRC) Convair-580 (CV580) during AIRS2. Liquid water content (LWC) and droplet number concentrations ( $N_d$ ) were obtained from hot-wire probes (Nevzorov and King probes) and Forward Scattering Spectrometer Probes

-----  
<sup>1</sup>Corresponding author: Ismail Gultepe, Cloud Physics and Severe Weather Research, Division, Environment Canada, Toronto, Ontario, M3H5T4, Canada; E-mail: ismail.gultepe@ec.gc.ca

(FSSP100), respectively.  $N_d$  and ice crystal number concentration ( $N_i$ ) were obtained at a standard size range of 2–47  $\mu\text{m}$  and an extended size range of 5–95  $\mu\text{m}$  from two Particle Measuring Systems (PMS), FSSP100s and from PMS two-dimensional cloud (2D-C; 25–800  $\mu\text{m}$ ) and precipitation (2D-P; 200–6400  $\mu\text{m}$ ) probe measurements. FSSP100<sub>st</sub> (standard size range; <47  $\mu\text{m}$ ) and FSSP100<sub>ext</sub> (extended size range; >95  $\mu\text{m}$ ) are used to calculate  $R_{\text{eff, st}}$  and  $R_{\text{eff, ex}}$ , respectively. FSSP measurements were corrected for probe dead-time and coincidence. Uncertainties in LWC and  $N_d$  are estimated at about 15% and 30%, respectively. Under most circumstances, the Nevzorov probe LWC and total water content (TWC) measurements are accurate to within 10–15% (Cober et al., 2001). Temperature measurements were obtained from both Rosemount and reverse flow ( $T_a$ ) probes with an accuracy of about  $\pm 1^\circ\text{C}$ .

## 2.2 GOES Observations

GOES-12 imager radiances were analyzed to retrieve cloud particle phase, size, liquid water path (LWP), optical thickness, and top temperature ( $T_G$ ) (Minnis et al., 1995) each half hour at a nominal resolution of 4 km as described by Minnis et al. (2004). For comparisons, the GOES cloud parameter values are computed as the weighted average of the retrievals for the four pixels closest to the aircraft coordinates. The (spatial) standard deviation is based on a weighted distribution of the closest pixel and the 8 surrounding pixels. Cloud particle phase, droplet effective size  $R_{\text{eff}}$ , and LWP were also averaged over an area defined by a 20-km radius circle centered on the surface site.

## 2.3 MWR and Precipitation Measurements

Two microwave radiometers, MWR1100 (22 and 30 GHz, 1 cm) and TP3000 (22 to 30 GHz and 51 to 59 GHz, 12 channels), representing integrated liquid water path (LWP) and profiling LWC measurements, were deployed at Mirabel, Quebec (47:32:43N; 70:04:07W) during the field program. The MWR1100 data provided estimates of LWP and integrated vapor mixing ratio ( $q_v$ ) in the column, and the TP3000 measured LWC,  $T$ , and  $q_v$  profiles. The data collected represent 1-minute averages of measurements taken every 20 seconds. The  $T$  accuracy is about 0.5 K with a precision of 0.25 K. Instrument details can be found in the MWR manual at [www.radiometrics.com](http://www.radiometrics.com). Presently, MWR measurements are used for indication of liquid regions within the cloud.

The surface precipitation type, e.g. snow or rain, was measured by the Precipitation Occurrence Sensor System (POSS, Sheppard and Joe, 1994) and reported by hourly surface observations at Mirabel. Its measurements together with conventional observations were assigned to time segments and were used to indicate when the MWR LWP measurements were likely to have been affected by precipitation. Precipitation-affected data are not used in the analysis.

## 3. METHOD

Discrimination between ice and liquid regions within the cloud was accomplished by using 1) a Rosemount icing detector (RID) which clearly responds to the liquid phase present within the cloud, and 2) FSSP and Nevzorov Probe measurements (Cober et al., 2001). Gultepe and Isaac (1997) provide a detailed summary of LWC and LWC fraction ( $k_L = \text{LWC}/(\text{LWC} + \text{IWC})$ ) versus  $T$  for climate studies.

The analysis of the aircraft data is performed in two ways. First, data along the aircraft flight track are analyzed to obtain effective radius ( $R_{\text{eff}}$ ), particle phase, LWC, IWC, and  $T$ . Second, LWC data over the Mirabel area are averaged over a physical thickness,  $dz=50$  m, to estimate LWP over the entire cloud. Using these data,  $R_{\text{eff}}$  versus LWC, and  $R_{\text{eff}}$  versus  $N_d$  are obtained. The LWP values are not obtained along the flight tracks because the aircraft data were limited to the flight level and do not necessarily represent the entire extent of the cloud. Data from the Mirabel area are only used for LWP and  $T$  comparisons.

## 4. RESULTS

Results are summarized based on in-situ observations, GOES retrievals, and their comparisons.

### 4.1 In-situ observations

Figure 1 shows an example of the measurements taken from the CV580 during the flight on 6 February. The disagreements in the time series of LWC and TWC (Fig. 1a) show that the CV580 encountered mixed phase conditions several times during the flight. The LWC values from the FSSP for the original and extended size ranges (Fig. 1b) indicate that the large particles account for most of the cloud water content. The vertical air velocity fluctuations (Fig. 1c) show no apparent correlation with the other parameters. However, the droplet number concentrations in Fig. 1d appear to increase when the Rosemount Icing Detector (RID) voltage (Fig. 1e) fluctuates (indicating icing),

especially at lower altitudes and greater temperatures (Fig. 1f). Similar data sets were analyzed for all 22 flights to obtain values of  $R_{\text{eff}}$ , LWC, and LWP.

Figure 2 shows an example for the same case but compares the values of  $T_G$  (Fig. 2a) and  $R_{\text{eff}}$  (Fig. 2b) obtained from the GOES retrievals with their counterparts from the CV580. In general,  $T_G$  is colder than  $T_a$ , indicating that aircraft collected the data below the cloud top (Fig. 2a). However, at 21.25 and 22.25 UTC, the temperatures are nearly identical and the satellite and in situ probes should be measuring similar parts of the cloud. Figure 2b shows time series of  $R_{\text{eff}}$  from FSSP100<sub>st</sub> (FSSP96), FSSP100<sub>ext</sub> (FSSP124), and the GOES retrievals together with the RID voltage and ice crystal concentration based on total number strobes ( $N_{i\text{TNS}}$ ). The last two parameters are shown to delineate liquid segments and mixed phase conditions. When  $N_{i\text{TNS}}$  increases, the FSSP-based  $R_{\text{eff}}$  is almost doubled indicating ice contamination and exclusion from the comparisons. Note that the GOES observations were gathered approximately every 15 minutes while the in-situ sampling rate was  $1 \text{ s}^{-1}$ . The GOES effective size ( $R_{\text{eff,G}}$ ) values generally fall between the  $R_{\text{eff,st}}$  and  $R_{\text{eff,ex}}$  measurements or are in good agreement with  $R_{\text{eff,st}}$  when there are fewer large droplets as seen around 22 UTC.

#### 4.2 GOES retrievals for all flights

Figure 3 shows the large-scale distribution of several GOES-retrieved cloud parameters at 2015 UTC, 6 February. The LWP (Fig. 3a) over the project area ranged from 150 to  $600 \text{ g m}^{-2}$  for this case, while  $R_{\text{eff}}$  (Fig. 3b) varied from 7 to  $20 \mu\text{m}$ . The physical thickness (Fig. 3c) was estimated to be between 1 and 7 km. The LWC can be estimated from LWP by dividing by the physical thickness. These example images highlight the variability of clouds sampled by the aircraft.

Using all GOES retrieved parameters along the flight tracks, plots of  $R_{\text{eff}}$  versus LWC,  $R_{\text{eff}}$  versus LWP, and LWP versus T, were developed for the entire data set and are shown in Fig. 4. In this figure, each color represent a specific flight track. In Fig. 4a,  $R_{\text{eff}}$  reaches a maximum of  $30 \mu\text{m}$ . The outer boundaries for LWC and LWP (Fig. 4b) increase exponentially with increasing  $R_{\text{eff}}$ , reflecting the detectability limits (minimum) and the maximum optical depth (128) used in the retrieval models (Minnis et al., 1998). The rest of the data points appear to be randomly distributed between the boundaries. It is seen that the minimum

value of  $R_{\text{eff}}$  for this dataset is  $\sim 7 \mu\text{m}$  and smaller values are removed from the analysis.

Figure 4b shows that  $R_{\text{eff}}$  is not a strong function of LWP. Figure 4c shows LWP versus T where LWP is given on a log scale. Although a small trend of decreasing LWP with increasing T seems to be evident, the scatter in the data is quite large. IN this figure, LWP values for  $T < -28^\circ\text{C}$  are not shown due to large ice particle concentrations.

#### 4.3 Comparison of microphysical parameters for five flights

The results for five selected cases are summarized in Fig. 5. The satellite LWP values do not show a good correlation with T (Fig. 5a), consistent with the results in Fig. 4. There appears to be some relationship between  $R_{\text{eff}}$  and LWC (Fig. 5b) for the 19 November and 6 February cases, but in general no trend is observed. Figure 5c shows a weak relationship where  $R_{\text{eff}}$  generally increases with increasing LWP. The corresponding values from the in-situ observations for the same flights are shown Fig. 6a. This figure was developed assuming the LWC fraction rate is  $> 0.90$  as measured using the Nevzorov probe. It is clearly seen that  $R_{\text{eff}}$  increases with increasing LWC for each flight. However, the overall scatter is similar to that seen in Fig. 5c. There are some contributions from the ice particles, evident for  $\text{LWC} < 0.02 \text{ g m}^{-3}$ . Figure 6b shows that  $R_{\text{eff}}$  is inversely proportional to  $N_d$  as expected from theoretical considerations.

#### 4.4 LWP comparisons at Mirabel

Figure 7 shows that MWR-based LWP at Mirabel can be determined even when  $T_G$  is less than  $-30^\circ\text{C}$  accounting for about 25% of the data points. These results indicate that ice clouds obscure the GOES view of the water clouds in about 25% of the cases. These conditions are denoted as indeterminate (shown in gray in Fig. 3a). Most of the GOES-based icing data points are found when  $T_G > -22^\circ\text{C}$ . If all of the LWP obscured by ice clouds was supercooled, then the satellite would be missing up to 25% of the possible icing cases.

Figure 8 shows the LWP versus T for both in-situ and GOES data. The fits obtained using binned T values are also shown. Trends for both data sets show that positive correlations exist with a weak correlation coefficient of about 0.6, and the relative error can be about more than 50%. As  $T_G$  decreases, the likelihood for ice clouds occurring over the water clouds increases, so the relationship should be weakest at the lower temperatures. The increased scatter at the coldest conditions is

consistent with the disconnect between  $T_G$  and LWP when ice clouds are present.

## 5. DISCUSSIONS

The results indicate that mixed phase clouds cannot be studied based on only GOES-based remote sensing methods. In-situ data can be used to validate remote sensing retrievals, but care must be taken to ensure that both sensors view the same cloud parts. GOES retrievals clearly are needed to study cloud top characteristics, but for deep cloud systems, integration of observations from satellites, models, parameterizations, and radars are invaluable.

Some ice contamination in the FSSP100 measurements can occur in mixed phase conditions causing some  $R_{\text{eff}}$  discrepancies. A more quantitative comparison of the GOES and aircraft observations will require combining data from both FSSPs and 2DC optical probes to compute the overall effective droplet radius. This reason can partially explain differences in  $R_{\text{eff}}$  obtained from satellite and in-situ based observations. When large super cooled liquid droplets (SLD) are present, it is clear that FSSP-based effective size calculations cannot be used to verify the remote sensing retrievals.

## 6. CONCLUSIONS

The main conclusions derived from the present work can be given as:

- ◆ In-situ  $R_{\text{eff}}$  values can be highly inaccurate when mixed phase conditions exist and instrumental size intervals do not reach the maximum particle size.
- ◆ High-level ice clouds can obscure the low-level clouds, and reflectivity fields represent only the integrated cloud conditions, not just the liquid part of the cloud. Therefore, under these circumstances, satellite retrievals cannot be used alone to detect icing conditions.
- ◆ If only FSSP measurements are used for in-situ  $R_{\text{eff}}$  calculations, the GOES-based retrievals will typically be larger than the in-situ values.
- ◆ The averaging scales can be important for comparisons and integration methods.
- ◆ MWR-derived LWP values should be used for validation of satellite retrievals because the measurements can be processed to represent the corresponding time scales for GOES data.

These conclusions show that an integration of observations is needed to better understand icing processes and to detect icing environments. A winter weather system being developed at Environment Canada named the Airport Vicinity Icing and Snow Advisor (AVISA), will integrate various products to assist in identifying and diagnosing icing conditions (Isaac et al., 2005b).

## Acknowledgments

Funding for this work was provided by Environment Canada, Transport Canada, the National Search and Rescue Secretariat of Canada, and the FAA. The satellite analyses were funded by the NASA Aviation Safety Program through the NASA Advanced Satellite Aviation-weather Products Initiative.

## REFERENCES

- Cober, G., G. A. Isaac, A. V. Korolev, and J. W. Strapp, 2001: Assessing cloud-phase conditions, *J. Appl. Meteor.*, 40, 1967-1983.
- Glazer, A. and G. A. Isaac, 2004: Forecasting icing conditions during Alliance Icing Research Study II with the Canadian Meteorological Center Global Environmental Multi-scale Model, 14th *International Conference on Clouds and Precipitation - ICCP2004*, Bologna, Italy. Accepted.
- Gultepe, I., G. A. Isaac, J. Key, J. Intrieri, D. O' C Starr, and K. B. Strawbridge, 2004: Dynamical and microphysical characteristics of the Arctic clouds using integrated observations collected over SHEBA during the April 1998 FIRE.ACE flights of the Canadian Convair. *Meteorology and Atmospheric Physics*, 85, 235-263.
- Gultepe, I., and Isaac, G. A., 1997: Relationship between liquid water content and temperature based on aircraft observations and its applicability to GCMs. *J. Climate*. 10, 446-452.
- Gultepe, I., and G. A. Isaac, 2004: An analysis of cloud droplet number concentration ( $N_d$ ) for climate studies: Emphasis on constant  $N_d$ . *Q. J. Royal Met. Soc.*, 130, Part A, No. 602, 2377-2390.
- Isaac, G.A., S.G. Cober, J.W. Strapp, A.V. Korolev, A. Tremblay, and D.L. Marcotte, 2001: Recent Canadian research on aircraft in-flight icing. *Canadian Aeronautics and Space Journal*, 47, 213-221.
- Isaac, G.A., J.K. Ayers, M. Bailey, L. Bissonnette, B.C. Bernstein, S.G. Cober, N. Driedger, W.F.J. Evans, F. Fabry, A. Glazer, I. Gultepe, J. Hallett, D. Hudak, A.V. Korolev, D. Marcotte, P. Minnis, J. Murray, L. Nguyen,

- T.P. Ratvasky, A. Reehorst, J. Reid, P. Rodriguez, T. Schneider, B.E. Sheppard, J.W. Strapp, and M. Wolde, 2005a: First results from the Alliance Icing Research Study II. *AIAA 43rd Aerospace Sci. Meeting and Exhibit*, Reno Nevada, 11-13 January 2005, AIAA 2005-0252.
- Isaac, G.A., S. Cober, N. Donaldson, N. Driedger, A. Glazer, I. Gultepe, D. Hudak, A. Korolev, J. Reid, P. Rodriguez, J.W. Strapp and F. Fabry, 2005b: Nowcasting airport winter weather: AVISA tests during AIRS. *World Weather Research Program Symposium on Nowcasting and Very Short Range Forecasting*, Toulouse, France, 5-9 September 2005. Extended Abstract 5.13 on Symposium CD.
- Minnis, P., et al., 1995: Cloud Optical Property Retrieval (Subsystem 4.3). "Clouds and the Earth's Radiant Energy System (CERES) Algorithm Theoretical Basis Document, Volume III: Cloud Analyses and Radiance Inversions (Subsystem 4)", *NASA RP 1376 Vol. 3*, edited by CERES Science Team, pp. 135-176.
- Minnis, P., L. Nguyen, W. L. Smith, Jr., M. M. Khaiyer, R. Palikonda, D. A. Spangenberg, D. R. Doelling, D. Phan, G. D. Nowicki, P. W. Heck, and C. Wolff, 2004: Real-time cloud, radiation, and aircraft icing parameters from GOES over the USA. *Proc. 13<sup>th</sup> AMS Conf. Satellite Oceanogr. and Meteorol.*, Norfolk, VA, Sept. 20-24, CD-ROM, P7.1.
- Sheppard, B.E., and Joe, P.I., 1994: Comparison of raindrop size distribution measurements by a Joss-Waldvogel Disdrometer, a PMS 2DG Spectrometer, and a POSS Doppler radar. *J. Atmos. Oceanic Technol.*, **11**, 874-887.

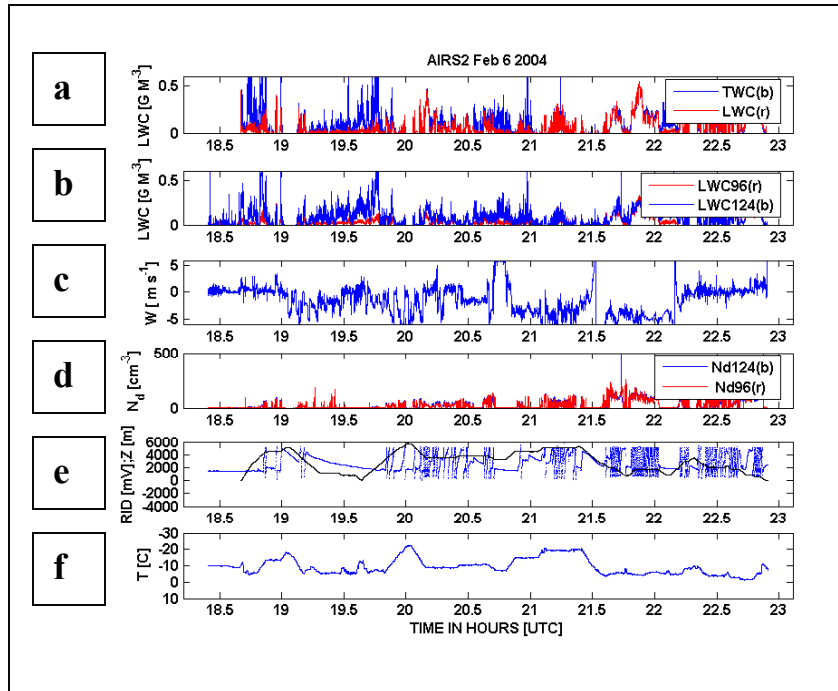


Fig. 1 Time series of LWC from hot wire probes, FSSP, vertical air velocity,  $N_d$ , height and RID voltage, and temperature for 6 February 2004.

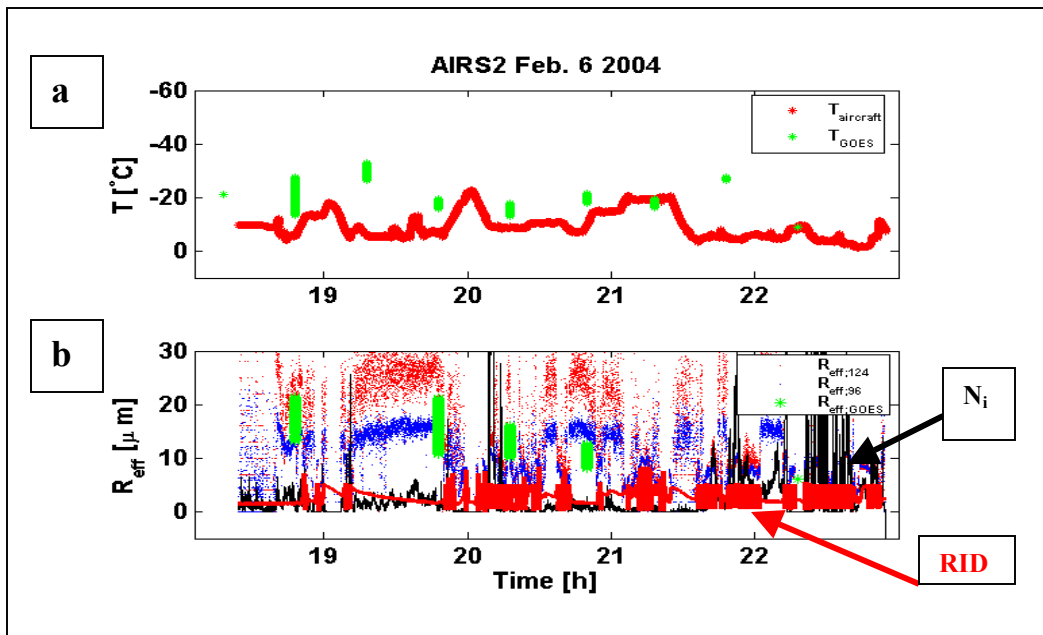


Fig. 2: Time series of  $T$  in box a, and  $R_{\text{eff}}$  in box b.  $N_i$  and RID values are shown with solid black line and red solid line, respectively, for indication of icing regions. The  $R_{\text{eff, st}}$  is represented by  $R_{\text{eff, 96}}$  and the  $R_{\text{eff, ex}}$  is represented by  $R_{\text{eff, 124}}$ .

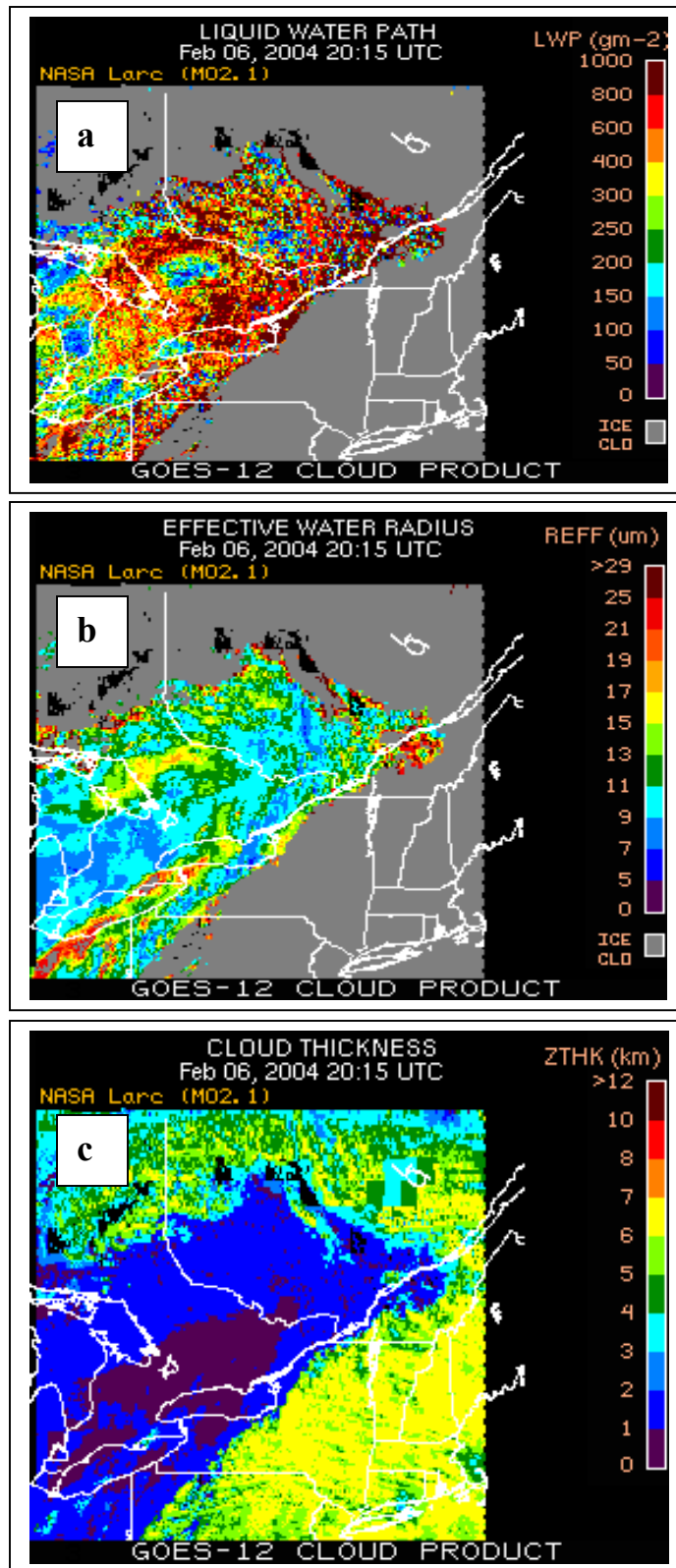


Fig. 3: Images of LWP,  $R_{\text{eff}}$ , and cloud physical thickness over the project area on Feb. 6 2005.

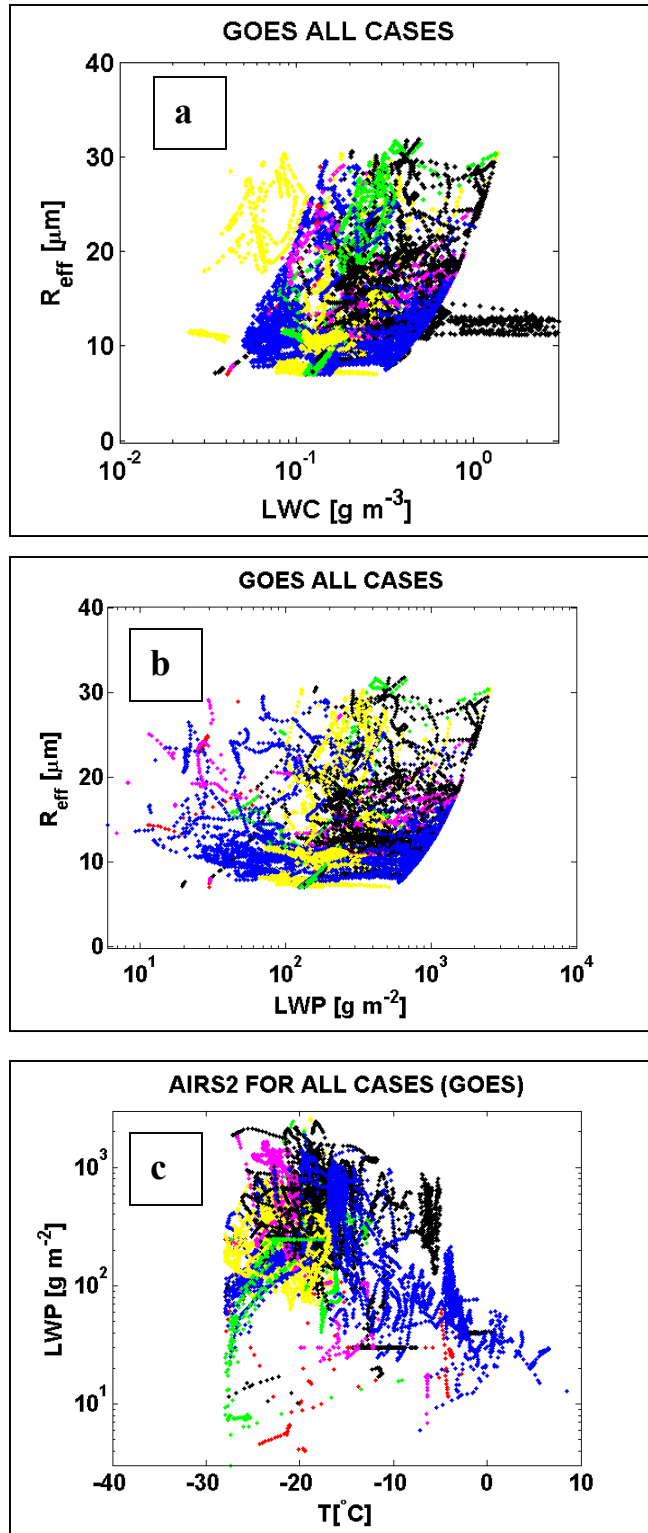


Fig. 4: Scatter plots of retrieved microphysical parameter along the flight tracks for entire project. Each color represents a flight track over 22 flights.

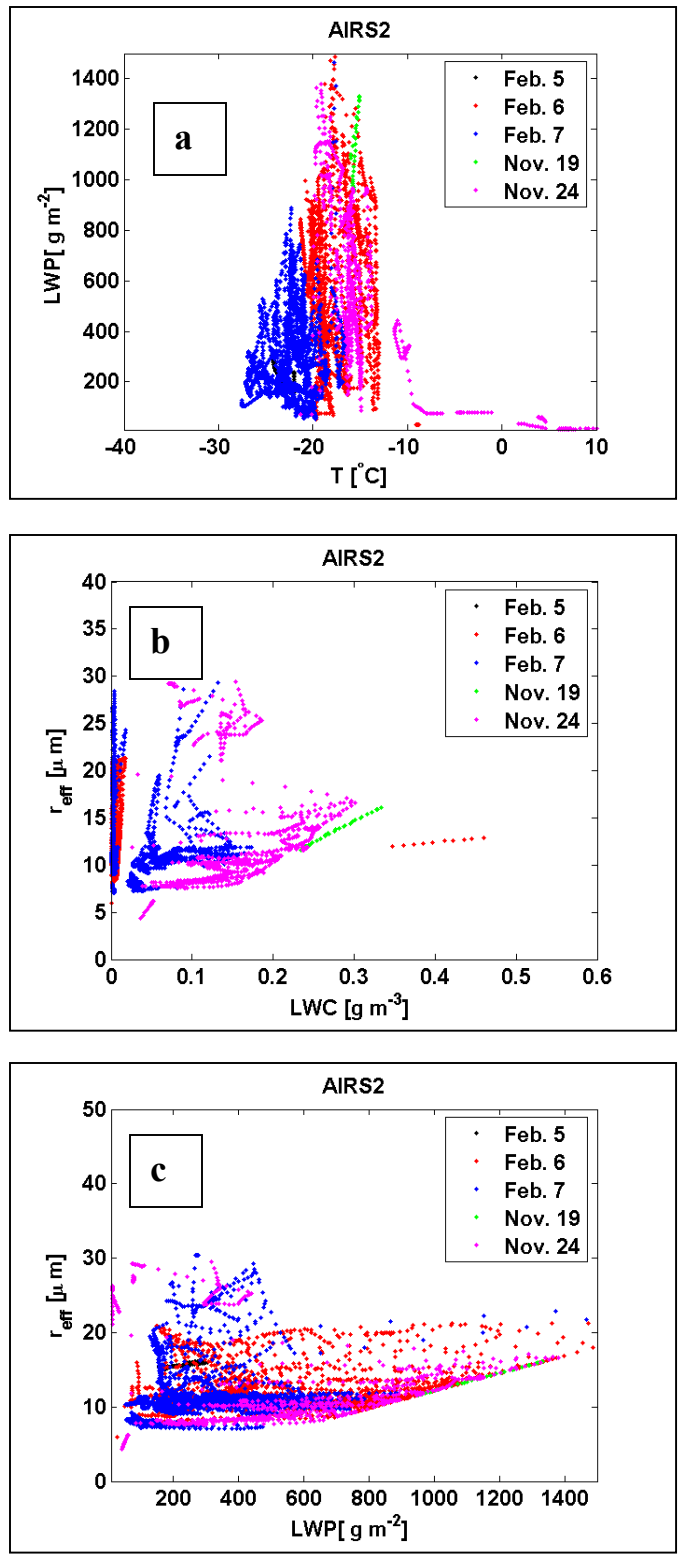


Fig. 5: Same as Fig. 4 but for the 5 flight cases shown on panel.

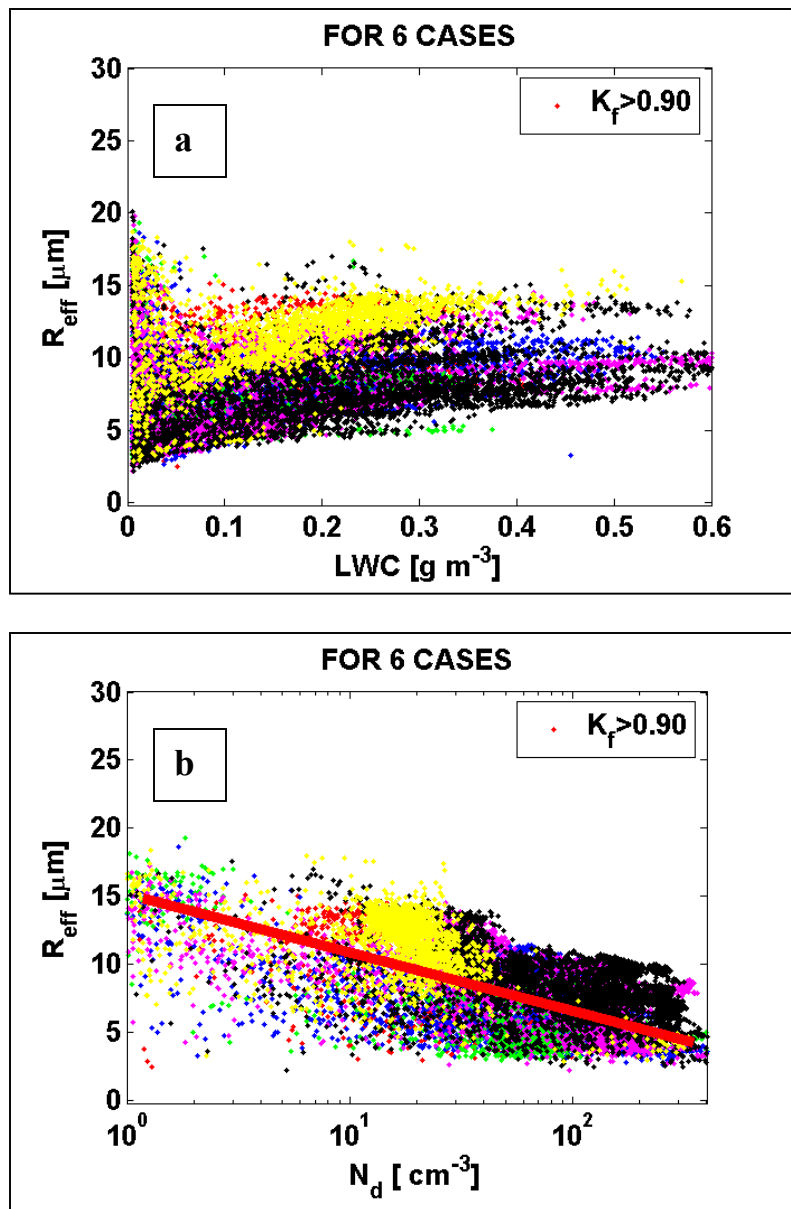


Fig. 6:  $R_{\text{eff}}$  versus LWC in box a, and  $R_{\text{eff}}$  versus  $N_d$  in box b. Each color represents a flight case as in Fig. 5. The red solid line represents the best fit applied to FSSP96.

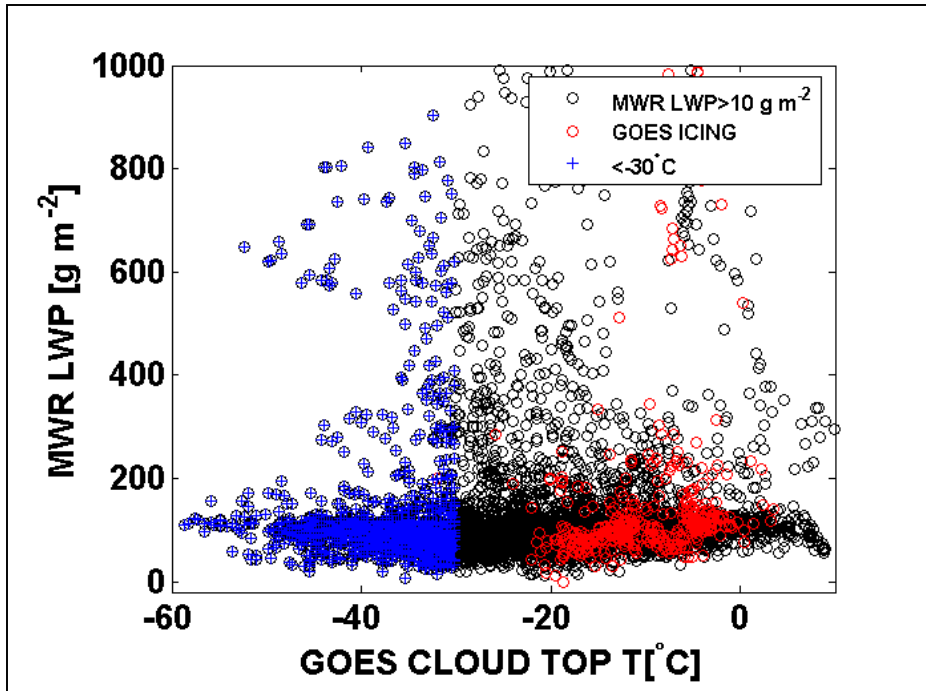


Fig. 7: MWR LWP versus GOES cloud top temperature. The red points are for icing conditions obtained from GOES observations.

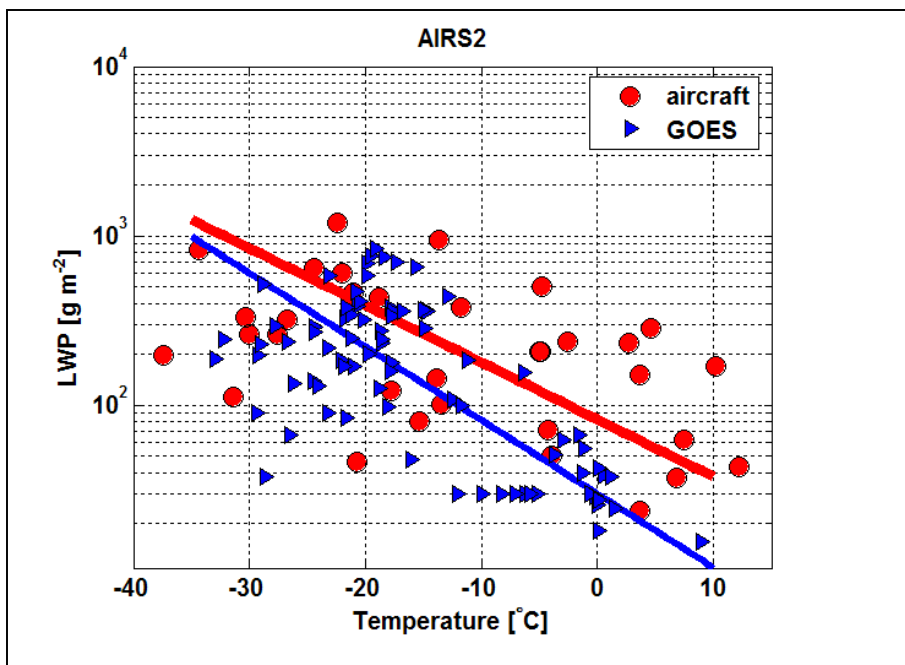


Fig. 8: LWP versus temperature. The solid lines are for fits using binned data. The redline represents  $y=82.41\exp(-0.0777x)$  for aircraft data and the blue line represents  $y=29.80\exp(-0.01001x)$  for GOES data. Aircraft based LWP is calculated over 50 m vertical intervals, and then integrated for entire cloud.